Sound wave propagation in transition-regime micro- and nanochannels

Nicolas G. Hadjiconstantinou
Department of Mechanical Engineering, Massachusetts Institute of Technology, Cambridge, Massachusetts 02139

(Received 27 November 2000; accepted 26 October 2001)

We present an extension of the existing continuum theory for sound wave propagation in dilute gases in ''narrow'' two-dimensional channels to arbitrary Knudsen numbers; the theory provides predictions for the wavelength and attenuation coefficient as a function of the oscillation frequency. A channel is considered narrow in the context of wave propagation when its height is much smaller than the characteristic diffusion length based on the wave frequency. This criterion is easily satisfied by small scale (transition-regime) channels for most frequencies of interest. Numerical simulations for a dilute monoatomic gas using the direct simulation Monte Carlo are used to verify the theoretical results. Good agreement is found between theory and simulation. © *2002 American Institute of Physics.* [DOI: 10.1063/1.1431243]

I. INTRODUCTION

In recent years much attention has been focused on fluid mechanics at the micrometer and submicrometer scale. As systems approach microscopic scales, increasing deviations from the well established continuum laws are reported.[1] In gas flows, the deviation from continuum behavior is quantified by the Knudsen number, $Kn=\lambda/H$, where λ is the molecular mean free path, and H is a characteristic lengthscale. For $Kn\gtrsim 0.1$, the continuum description is known to fail; the regime $0.1<Kn<10$ is known as the transition regime because it represents a transition between diffusive (continuum) molecular behavior for $Kn\lesssim 0.1$, and ballistic molecular behavior (free molecular flow) for $Kn\gtrsim 10$. Here, we focus on flows in two-dimensional channels which are the predominant building blocks in today's microfabrication techniques. The characteristic lengthscale H in this case is the channel height.

In this paper, we investigate the characteristics of axial plane waves in dilute gases in two-dimensional channels with heights that place them in the transition regime. Due to the small channel dimensions, we expect the system to fall within the ''narrow channel'' definition for most frequencies of interest. A channel is considered narrow with regard to wave propagation if the diffusion length based on the oscillation frequency is much larger than the channel height, that is, if the ratio $\delta=\sqrt{2\nu/\omega}/H$ is much larger than unity, where ν is the kinematic viscosity and ω is the wave angular frequency. This requirement is easily met in transition regime flows if we assume that the neglect of inertial effects in the transition regime is governed by a criterion similar to the one above. Consider gaseous argon at atmospheric pressure as an example: At $Kn=0.1$, any frequency $\omega<10^7$ rad/s leads to narrow channel behavior; at $Kn=10$, the narrow channel approximation is valid for any frequency $\omega<10^{11}$ rad/s.

Solution to this problem is obtained by using a method devised by Lamb to investigate wave phenomena in the narrow channel limit in the continuum case.[2,3] This method allows the determination of the wave propagation constant without explicitly solving for the velocity field inside the channel; only information about the steady-state bulk flowrate in response to a constant pressure gradient is required. Lamb's method is based on the realization that for narrow systems as defined above, times long compared to the system's diffusive time scale are still very short compared to the characteristic time of oscillation. This allows the coarse graining of the time description to the diffusive time scale of the system; in the resulting description, the effects of inertia are negligible and a diffusion equation is obtained[2] that governs the *steady-state* oscillatory behavior of the system. The paradox of a diffusion equation, with its associated ''infinite'' disturbance propagation speed, describing the wave propagation characteristics of the system is resolved by recalling that time has been coarse grained over the time required to establish the diffusive effects and the time derivative associated with inertial effects has been dropped, leading to an approximation that does not capture the transient propagation of disturbances for times shorter than the viscous diffusion time. The terms ''wave propagation'' and ''complex propagation constant'' are used here for historical reasons, and it is implied throughout the paper that their use refers to the steady-state response of the system (wavelength and attenuation coefficient) under oscillatory forcing.

Lamb's method yields identical results for narrow channels[3] to the full theory of wave propagation in the continuum regime as developed by Kirchhoff[4] since the approximations involved are consistent and physically correct. Here we utilize the fact that the propagation constant can be evaluated without explicitly solving for the velocity field inside the channel, to provide predictions for the wave propagation constant in the transition regime that would otherwise require solution of the Boltzmann equation.

The theoretical predictions are verified using direct Monte Carlo simulations (DSMC).[5] In all of the following work we have used the hard-sphere gas model since for the verification and method demonstration purposes of this paper, it is preferable to use a model for which ample numeri-

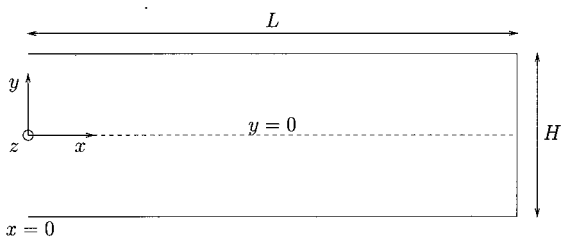

FIG. 1. Channel geometry. The walls at $y=-H/2, H/2$ are diffuse, and the wall at $x=L$ is specular.

cal and theoretical results exist and the DSMC method is guaranteed to be exact. As will be clear in the next section, the development of the theory is in no way dependent on the exact intermolecular force law. Additionally, the hard-sphere model has been shown to capture average flow rates of real gases in tubes and channels reasonably well.[6,7] Transport coefficient dependence on temperature is not an issue, since the thermal diffusion length will also be large compared to the channel height (in gases $Pr\sim 1$) and thus the flow will be isothermal. Simulations in the range $0.3<\delta<24$ verify the theoretical result, but also show that the latter, strictly valid for $\delta\gg 1$, can be considered valid at less extreme values of δ than one would originally expect.

II. THEORY FOR WAVE PROPAGATION IN NARROW CHANNELS

A. Continuum theory

We now give a fairly detailed outline of the theory for plane wave propagation in narrow channels and ducts in the continuum limit, first developed by Lamb.[2,3] We extend this theory to the transition regime in the next section.

We consider two-dimensional smooth channels of length L with perfectly accommodating walls that are a distance H apart (see Fig. 1). The gas velocity field is denoted $\mathbf{u}=\mathbf{u}(x,y,t)=[u(x,y,t),v(x,y,t),w(x,y,t)]$. For long channels ($L\gg H$), the velocity in the direction normal to the walls is negligible and the pressure is uniform across any section of the channel $[P=P(x,t)]$. In this case the linearized equation for momentum conservation is given by

$$\rho\frac{\partial u}{\partial t}=\mu\frac{\partial^2 u}{\partial y^2}-\frac{\partial P}{\partial x}, \tag{1}$$

where ρ is the average gas density, and μ is the gas viscosity. Under an excitation of the form $\exp(i\omega t)$, a response of the form $u(x,y,t)=\tilde{u}(x,y)\exp(i\omega t)$, $P(x,t)=\tilde{P}(x)\exp(i\omega t)$ is expected. The amplitudes $\tilde{u}$ and $\tilde{P}$ are governed by

$$i\rho\omega\tilde{u}-\mu\frac{\partial^2\tilde{u}}{\partial y^2}=-\frac{d\tilde{P}}{dx}, \tag{2}$$

or

$$\frac{\partial^2\tilde{u}}{\partial y^2}+\phi^2\tilde{u}=\frac{1}{\mu}\frac{d\tilde{P}}{dx}, \tag{3}$$

where $\phi^2=-i\rho\omega/\mu$. The solution of this equation subject to a symmetry condition at the channel centerline and no slip at the walls is

$$\tilde{u}=\frac{1}{\mu\phi^2}\frac{d\tilde{P}}{dx}-\frac{\cos\phi y}{\mu\phi^2\cos\frac{\phi H}{2}}\frac{d\tilde{P}}{dx}. \tag{4}$$

A solution in terms of the bulk velocity in now sought; this approach reduces the problem into a one-dimensional one, with the help of the concept of the channel resistance $\mathcal{R}$, defined in the equation below. The amplitude of the bulk velocity associated with the above response is

$$\tilde{u}_b=\frac{1}{H}\int_{-H/2}^{H/2}\tilde{u}\,dy=\frac{1}{\mu\phi^2}\frac{d\tilde{P}}{dx}-\frac{2}{\mu\phi^3 H}\frac{d\tilde{P}}{dx}\tan\frac{\phi H}{2}$$

$$\equiv-\frac{1}{\mathcal{R}}\frac{d\tilde{P}}{dx}. \tag{5}$$

As $|\phi H/2|\to 0$ the effect of inertia becomes negligible and the bulk flow rate reduces to the Poiseuille expression

$$\tilde{u}_b=-\frac{H^2}{12\mu}\frac{d\tilde{P}}{dx}. \tag{6}$$

The condition $|\phi H/2|\to 0$ is of course equivalent to the narrow channel requirement $\delta=\sqrt{2\nu/\omega}/H\gg 1$ that was developed in Sec. I through physical reasoning. This result shows that in the absence of inertia, the wave propagation problem is governed by the steady-state flow characteristics of the channel.

The final step to determining the wave propagation characteristics is the substitution of the pressure gradient in terms of the fluid particle displacement ξ, where

$$u(x,y,t)=\frac{\partial\xi(x,y,t)}{\partial t} \tag{7}$$

and

$$u_b(x,t)=\tilde{u}_b(x)\exp(i\omega t)=\frac{1}{H}\int_{-H/2}^{H/2}\frac{\partial\xi(x,y,t)}{\partial t}dy$$

$$=\frac{\partial\overline{\xi}(x,t)}{\partial t}. \tag{8}$$

If T is the gas temperature, for isothermal changes (narrow channel)[2,4]

$$\frac{\partial P}{\partial x}=-\left(\frac{\partial P}{\partial\rho}\right)_T\rho\frac{\partial^2\xi}{\partial x^2}. \tag{9}$$

Equation

$$\tilde{u}_b=-\frac{1}{\mathcal{R}}\frac{d\tilde{P}}{dx}, \tag{10}$$

can thus be written as

$$\frac{\partial\overline{\xi}}{\partial t}=\frac{P}{\mathcal{R}}\frac{\partial^2\overline{\xi}}{\partial x^2}. \tag{11}$$

The complex propagation constant $\beta\,[u_b \propto \exp(-\beta x)]$ is thus given by[2,3]

$$\beta^2 \equiv (\alpha + ik)^2 = i\omega\mathcal{R}/P, \tag{12}$$

where $k = 2\pi/\lambda = \omega/c$ is the wave number, λ is the wavelength, c is the sound speed, and α is the attenuation coefficient. If we substitute $\mathcal{R} = 12\mu/H^2$ we obtain the well-known result

$$\beta^2 = \frac{12i\omega\mu}{PH^2}, \tag{13}$$

for wave propagation in narrow channels that was originally obtained by taking the limit of a narrow channel in Kirchhoff's general theory.[4]

The assumption of isothermal flow, motivated here through physical reasoning, has been verified by Kirchhoff's general theory[4] which includes the effects of heat conduction. Kirchhoff's theory shows[3] that the normalized temperature variation relative to the normalized velocity amplitude is proportional to δ^{-1} and thus negligible in narrow channels.

B. Transition regime

We now turn to wave propagation in the transition regime. We make use of the fact that equation

$$\frac{\partial P}{\partial x} = -\left(\frac{\partial P}{\partial \rho}\right)_T \rho \frac{\partial^2 \xi}{\partial x^2},$$

is a kinematic condition and thus applicable in all Knudsen regimes. The more general form of momentum conservation valid for all Knudsen regimes requires

$$i\rho\omega\tilde{u} - \frac{\partial \tilde{\tau}_{xy}}{\partial y} = -\frac{d\tilde{P}}{dx}, \tag{14}$$

where $\tilde{\tau}_{xy}$ is the xy component of the amplitude of the stress tensor. When inertia is negligible, the equation reduces to

$$\frac{\partial \tilde{\tau}_{xy}}{\partial y} = \frac{d\tilde{P}}{dx}, \tag{15}$$

which shows that, similarly to the continuum case, the wave propagation characteristics are governed by the steady-state flow characteristics of the channel. Despite the breakdown of continuum theory in the transition regime, we will continue to use $\delta \gg 1$ as the criterion for negligible inertia and narrow-channel behavior. As will be seen in the results section, this remains an accurate, if slightly conservative, measure.

It has been shown[6,8,9] that in the linear steady-flow regime there exists a flow resistance $\mathcal{R} = \mathcal{R}(Kn)$ defined by

$$\tilde{u}_b = -\frac{1}{\mathcal{R}(Kn)}\frac{d\tilde{P}}{dx}, \tag{16}$$

that describes the flow rate in channels for all Knudsen numbers; this resistance can be determined by experiments,[6–8] linearized solutions of the Boltzmann equation,[6,7,9] or molecular simulations.[7]

Knowledge of the flow resistance $\mathcal{R}(Kn)$ allows the calculation of the propagation constant with no reference to the exact flow profile inside the channel as shown in the previous section: Combining Eqs. (9) and (16), we obtain the counterpart of Eq. (11) governing wave propagation in narrow channels in all Knudsen regimes

$$\frac{\partial \overline{\xi}}{\partial t} = \frac{P}{\mathcal{R}(Kn)}\frac{\partial^2 \overline{\xi}}{\partial x^2}. \tag{17}$$

Thus for a narrow channel the complex propagation constant in the absence of inertia effects is given by

$$\beta^2 \equiv (\alpha + ik)^2 = i\omega\mathcal{R}(Kn)/P, \tag{18}$$

for all Knudsen numbers, provided the flow resistance is an appropriate function of the Knudsen number. The specific functional form of $\mathcal{R}(Kn)$ is of no consequence as no assumptions have been made concerning its form or origin, except that it describes flow in the linear regime.

Here we use the following scaling relation valid for all Knudsen numbers[6,9,10] to describe the flowrate in pressure-driven flow

$$\dot{Q} = \tilde{u}_b H = -\frac{1}{P}\frac{d\tilde{P}}{dx}H^2\sqrt{\frac{RT}{2}}\overline{Q}, \tag{19}$$

and thus identify an expression for the flow resistance $\mathcal{R}(Kn)$ which is valid for all Knudsen numbers. Here $R = k_b/m_m$ is the gas constant, k_b is Boltzmann's constant, m_m is the molecular mass, and $\overline{Q} = \overline{Q}(Kn)$ is a proportionality coefficient that can be determined by molecular simulation or experiment.[6] For the purposes of comparison with our hard-sphere DSMC calculations, we will use $\overline{Q}(Kn)$ as determined by solution of the linearized Boltzmann equation [9] for flow of a hard sphere gas in a two-dimensional channel. In the transition regime, $\overline{Q}(Kn)$ varies slowly about its minimum value $(1.5 \lesssim \overline{Q}(0.1 < Kn < 10) \lesssim 3)$ occurring at $Kn \approx 1$. For real gas applications, appropriate values of $\overline{Q}(Kn)$ that describe real-gas behavior need to be used.

From Eq. (19) we can identify

$$\mathcal{R}(Kn) = \frac{P}{H\overline{Q}\sqrt{RT/2}}, \tag{20}$$

leading to

$$c = \sqrt{2\omega H\overline{Q}\sqrt{RT/2}} \tag{21}$$

and

$$\alpha = \sqrt{\frac{\omega}{2H\overline{Q}\sqrt{RT/2}}}. \tag{22}$$

These expressions are expected to hold in all Knudsen regimes since both ingredients, Eqs. (9) and (19), are valid in all Knudsen regimes. These predictions are shown below to be in agreement with direct Monte Carlo simulations of wave propagation in narrow channels.

III. SIMULATION OF WAVE PROPAGATION

A. Numerical technique

We simulated gaseous argon (molecular mass $m_m = 6.63\times10^{-26}$ kg, hard-sphere diameter $\sigma = 3.66\times10^{-10}$ m) in a two-dimensional channel using standard DSMC techniques.[5,11] We considered fully accommodating walls; our simulations will thus be compared with the theoretical results using values of $\bar{Q}$ derived for fully accommodating walls. The average gas pressure and temperature were $P = 1.013\times10^5$ Pa, and $T = 273$ K, respectively, leading to a mean free path $\lambda = m_m/(\sqrt{2}\pi\sigma^2\rho) \approx 6.25\times10^{-8}$ m. The choice of species should have no effect on our nondimensionalized results that should apply to any dilute hard-sphere gas.

In the sake of brevity we will not present a description of the DSMC algorithm. Excellent introductory[11] and detailed[5] descriptions can be found in the literature; comparisons of DSMC simulation results with solutions of the linearized Boltzmann equation and experimental results for diverse nonequilibrium phenomena spanning the whole Knudsen range can be found in Refs. 5 and 12.

Sound waves are excited by imposing a sinusoidally varying particle influx at $x=0$. Our simulations have shown that the particle influx generates a *pressure* disturbance in the simulation domain that is subsequently propagated. The varying particle influx can be generated by a varying velocity in the x direction (the method used here) or a varying density; both methods yield identical results. The pressure disturbance at $x=0$ is imposed using the well-known Maxwellian reservoir method: Particles exiting the domain at $x=0$ are discarded, whereas particle influx is accounted for by a reservoir attached to the simulation domain at $x=0$ and extending to $x=-L_R$. Each time step, particles at the required density (sinusoidally varying in time in the variable-density case) are generated inside the reservoir and are given velocities drawn from a Maxwellian distribution at the simulation temperature. The Maxwellian distribution has a time-dependent mean velocity in the x direction that is equal to the desired velocity (sinusoidally varying in time in the variable-velocity case). The particle positions are advanced in time (one time step Δt); the particles that cross the plane $x=0$ and enter the simulation domain represent the half-space Maxwellian influx and are retained. The particles remaining in the reservoir are discarded and the simulation proceeds as usual. The length of the reservoir is set to $L_R = v_{\text{cutoff}}\Delta t$, where $v_{\text{cutoff}} = 6\sqrt{2k_bT/m_m}$ is a velocity for which the probability (based on a Maxwellian distribution) is very small.

In order to minimize the cost of our simulations, the domain length, L, was taken to be of the order of one wavelength. The far end of the domain ($x=L$) was terminated by a specular wall. In the absence of dissipation, the system would exhibit pure standing waves. In the present case, the reflected wave amplitude was negligible due to the high dissipation associated with narrow channels.

More than 30 (on average) molecules per cell were used to ensure accurate solutions. The transport coefficients in DSMC are known[13] to deviate from the dilute gas Enskog values as the square of the cell size Δx with the proportionality constant such that for cell sizes of the order of one mean free path, the error is of the order of 10%. To minimize this error, we used three cells per mean free path for $H>3\lambda$, but the number of cells per mean free path was increased for smaller systems to ensure that there were at least eight cells across the channel width. It has been shown[14,15] that the error in the transport coefficients is proportional to the square of the time step, with the proportionality constant such that for time steps of the order of one mean free time, the error is of the order of 5%. The error due to a finite time step Δt is negligible in our simulations; the time step was taken to be significantly smaller than the mean free time λ/c_o [in fact, $\Delta t < \lambda/(5c_o)$] where $c_o = \sqrt{2k_bT/m_m}$ is the most probable velocity.

Temperature variations due to dissipation were closely monitored, and the mean temperature was found to deviate at most by 2%. A variation of this magnitude leads to a change of at most 1% in the adiabatic–isothermal sound speed and continuum transport coefficients, given that these vary as $\sqrt{T}$. We expect temperature effects in the transition regime studied here to be similarly small.

The reservoir forcing was chosen such that the resulting wave amplitude, u_{oo}, was small to avoid nonlinear effects. Our simulations have been performed with a wave amplitude $u_{oo} \approx 0.02c_s$ that has been found, as discussed below, to be sufficiently small. Here $c_s = \sqrt{\gamma k_bT/m_m}$ is the adiabatic sound speed and γ is the ratio of the specific heats. In the continuum regime, the ratio between the viscous and nonlinear inertial terms scales as $(\mu u_{oo}/H^2)/(\rho u_{oo}^2/\ell)$. This scaling indicates viscous effects dominate nonlinear inertial effects if $u_{oo} \ll c\delta^2$. Although the continuum assumption breaks down in the transition regime, we will use this criterion as an indication of the importance of nonlinear inertial forces. Based on this criterion, we expect nonlinear effects to be negligible in all of our simulations. To verify this, we performed simulations at selected frequencies with $u_{oo} \approx 0.05c_s$ and $u_{oo} \approx 0.01c_s$, which produced results that were indistinguishable (within statistical fluctuations) from our original simulations with $u_{oo} \approx 0.02c_s$.

After the initial transients have passed, the value $u_b(x,t)$ was measured in the simulations at each time step in slices along the x axis. Our sampling method[16] accounts for the transient nature of the simulation (that leads to zero time averages), by using the fact that the bulk velocity time-dependence is of the following known form:

$$u_b(x,t) = u_{oo}[e^{-\alpha x}\sin\,\omega t\,\cos\,kx - e^{-\alpha x}\cos\,\omega t\,\sin\,kx] \equiv A(x)\cos\,\omega t + B(x)\sin\,\omega t. \tag{23}$$

The spatial dependence of the bulk velocity which contains the information about the attenuation coefficient and the wavelength, can be recovered from the simulation through the application of a chi-square fit[17] to the functional form of Eq. (23). The desired amplitudes $A(x)$ and $B(x)$ are given by

$$A(x_j) = \frac{\Sigma s^2 \Sigma uc - \Sigma sc \Sigma us}{\Sigma c^2 \Sigma s^2 - (\Sigma sc)^2}, \tag{24}$$

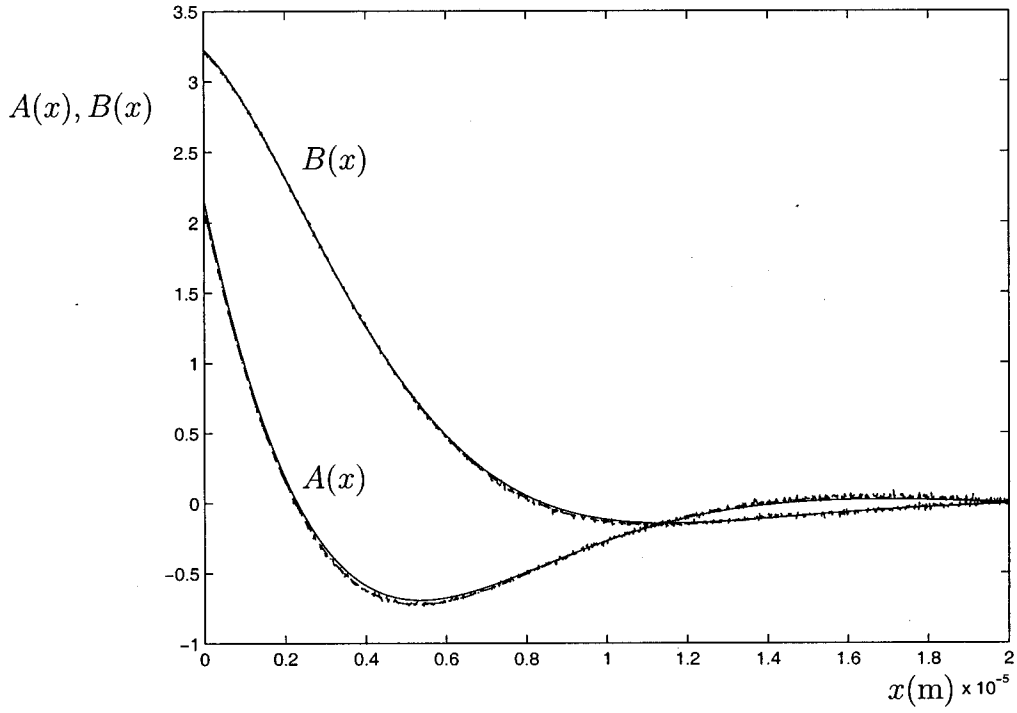

FIG. 2. Cosine and sine components, $A(x)$ and $B(x)$, of the velocity amplitude (in m/s) for $\omega=18.5\times10^6$ rad/s, $H=0.4$ μm. The smooth line indicates the expected solution based on Eqs. (21) and (22), and the jagged line is the molecular simulation result.

$$B(x_j)=\frac{\Sigma c^2\Sigma us-\Sigma sc\Sigma uc}{\Sigma c^2\Sigma s^2-(\Sigma sc)^2}, \tag{25}$$

where

$$\Sigma s^2=\sum_i^M \sin^2\,\omega t_i, \quad \Sigma c^2=\sum_i^M \cos^2\,\omega t_i,$$

$$\Sigma sc=\sum_i^M \sin\,\omega t_i\cos\,\omega t_i$$

$$\Sigma us=\sum_i^M u_b(x_j,t_i)\sin\,\omega t_i,$$

$$\Sigma uc=\sum_i^M u_b(x_j,t_i)\cos\,\omega t_i,$$

with x_j being the position of slice j along the x axis, and M being the number of time samples recorded. The Nelder–Mead simplex method[17] is used to perform a nonlinear chi-square fit of $A(x)$ and $B(x)$ to extract the wave number k and the attenuation coefficient α. A phase shift is also included in the parameter fits to allow for the phase difference between the enforced pressure disturbance and the observed velocity variation [see Eq. (16)], and entrance effects.

B. Simulation results

Our simulations were performed in the frequency range 0.25×10^6 rad/s$<\omega<18.5\times10^6$ rad/s. Since the simulation cost increases linearly with the simulated time which is proportional to the oscillation period $(2\pi/\omega)$, $\omega=0.25\times10^6$ rad/s was the lowest frequency we could simulate with our present computational resources.

An estimate for the magnitude of homogeneous absorption is given by the continuum formula that includes the effects of viscosity and thermal conductivity[18]

$$\alpha_h=\frac{\omega^2}{2\rho c_s^3}\left[\left(\frac{4}{3}\mu+\zeta\right)+\frac{\kappa}{c_p}(\gamma-1)\right]. \tag{26}$$

Here, c_p is the specific heat at constant pressure, κ is the thermal conductivity, and ζ is the coefficient of bulk viscosity which is equal to zero for an ideal gas. Based on this estimate, we find that homogeneous absorption in our simulations is expected to be negligible compared to the dissipation due to the wall presence [Eq. (22)]. High-frequency effects are also negligible at these frequencies.[19]

Figure 2 shows a typical simulation result for $A(x)$ and $B(x)$. Figures 3 and 4 show the comparison between the theoretical and simulation results for the sound speed and attenuation coefficient, respectively, in the frequency range 0.25×10^6 rad/s$<\omega<18.5\times10^6$ rad/s for a channel height $H=0.1$ μm. The agreement is very good.

We also performed simulations at $\omega=18.5\times10^6$ rad/s for a variety of channel heights. The results of these simulations plotted as functions of δ are shown in Figs. 5 and 6. These figures show that the narrow channel theory is valid for $\delta>1$ and is qualitatively correct even for $\delta\approx1$ despite the fact that it is expected to be valid only for $\delta\gg1$.

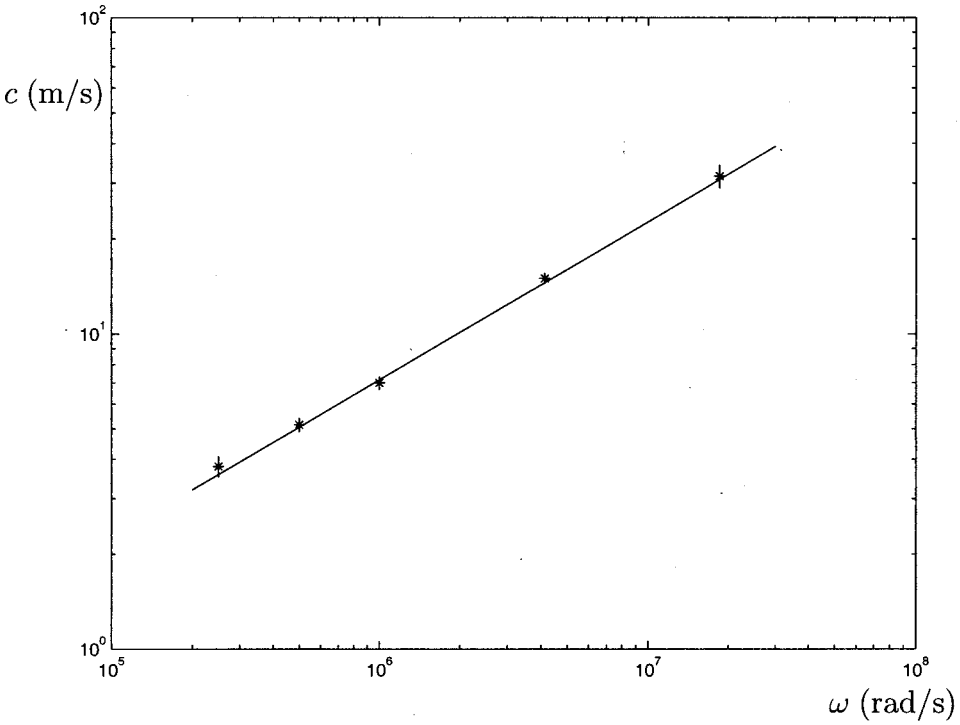

FIG. 3. Comparison between the theoretical prediction of Eq. (21) shown as a solid line and simulation results denoted by stars at a fixed channel height of $H=0.1$ μm.

IV. CONCLUDING REMARKS

The agreement between the theoretical expression for the complex propagation constant and DSMC simulations is very good. Our simulation results indicate that in the transition regime the narrow channel assumption can be considered valid for $\delta>1$, rather than the expected $\delta\gg1$. Our conclusions are also not affected by the use of a "sharper" criterion that compares the diffusion length to the channel half-height (2δ). The development of a transition-regime counterpart to the continuum-based measure, δ, may address the slightly conservative predictions of the current measure.

Although simulations were limited to the transition regime, the expressions presented are valid for arbitrary Knudsen numbers and are thus expected to be valid in the slip-flow and free molecular flow regimes. In the slip-flow regime, $\mathcal{R}(Kn)$ can be determined by the slip-flow corrected version of the Poiseuille formula $\mathcal{R}=12\mu/H^2$.

Extension of these results to tubes and ducts of arbitrary

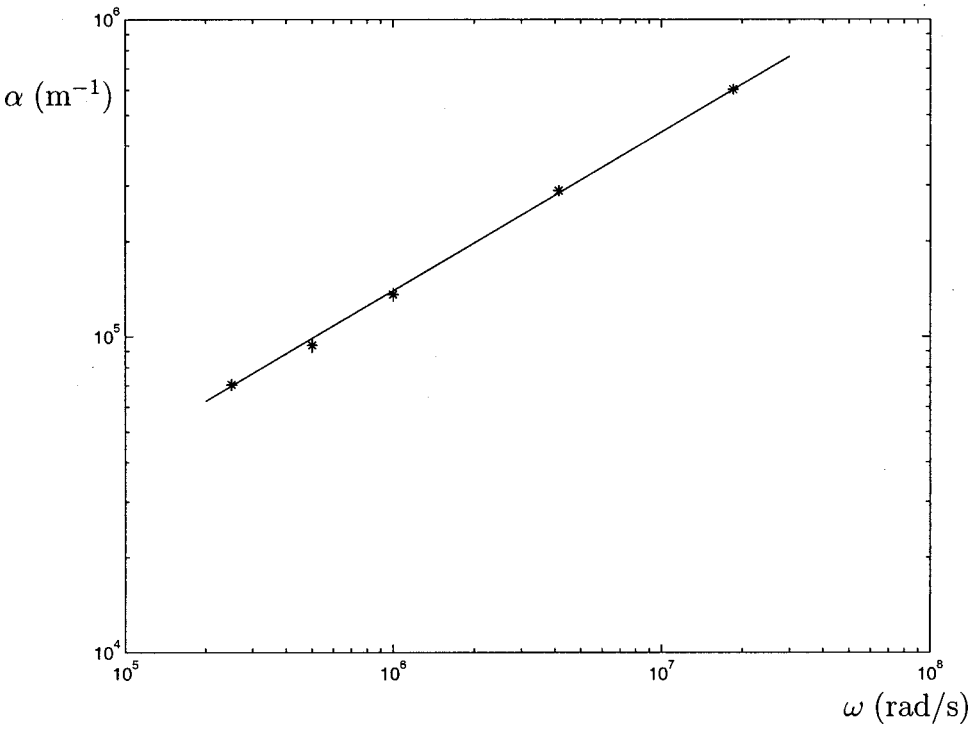

FIG. 4. Comparison between the theoretical prediction of Eq. (22) shown as a solid line and simulation results denoted by stars at a fixed channel height of $H=0.1$ μm.

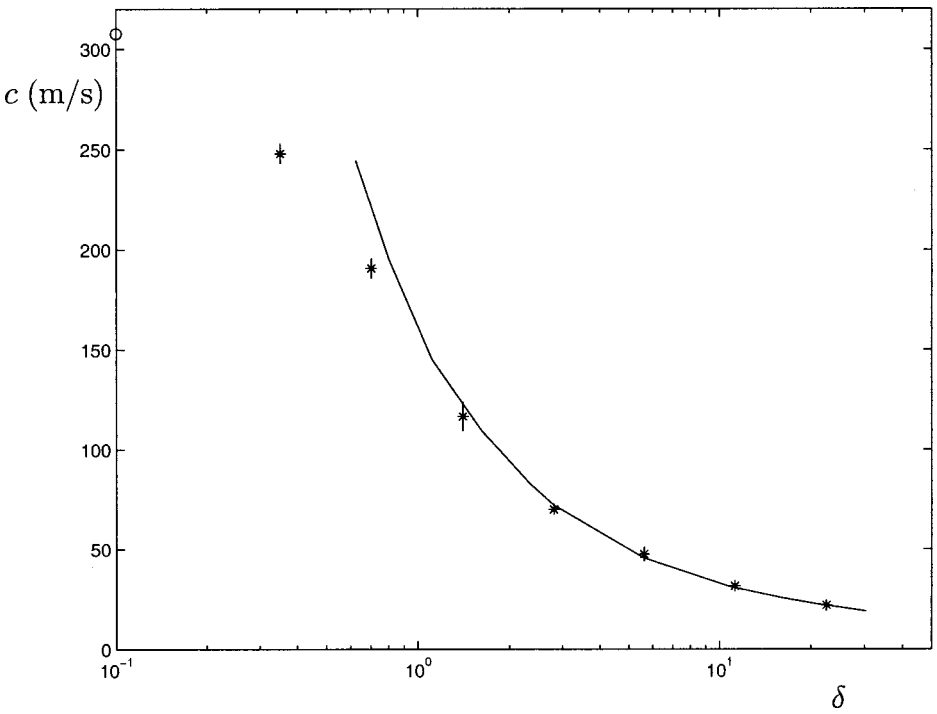

FIG. 5. Comparison between the theoretical prediction of Eq. (21) shown as a solid line and the simulation results at a fixed frequency ($\omega = 18.5 \times 10^6$ rad/s) denoted by stars. The open circle denotes the sound speed in the absence of walls ($\delta = 0$).

cross-section directly follows. Although in this work we used the dilute hard-sphere gas model, we expect the results to approximate real monoatomic gas behavior well. Comparison with experiments shows that the pressure-driven flowrate in real gases can be captured fairly accurately by the dilute gas model.[6,7]

ACKNOWLEDGMENTS

The author wishes to thank Alej Garcia for help with the computations, helpful comments and discussions. The author is also indebted to Anthony Patera for helpful comments. This work was initiated while the author was visiting the Center for Applied Scientific Computing (CASC) at the Lawrence Livermore National Laboratory. The author would like to thank Xabier Garaizar for making this work possible through the computer resources made available to the author, and Dr. Kyran Mish, Director, Center for Computational Engineering, Lawrence Livermore National Laboratory, for financial support (U.S. Department of Energy, W-7405-ENG-48).

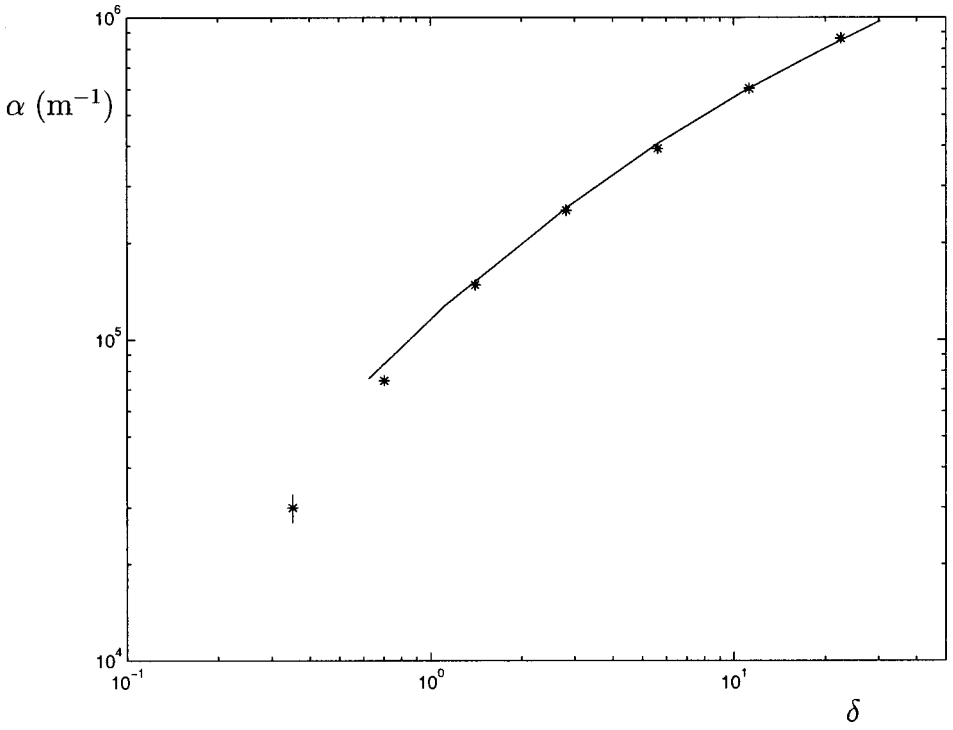

FIG. 6. Comparison between the theoretical prediction of Eq. (22) shown as a solid line and the simulation results at a fixed frequency ($\omega = 18.5 \times 10^6$ rad/s) denoted by stars. At this frequency, $\alpha_h \approx 160$ m^{-1}.

[1]C. M. Ho and Y. C. Tai, ''Micro-electro-mechanical systems (MEMS) and fluid flows,'' Annu. Rev. Fluid Mech. **30**, 579 (1998).
[2]I. B. Crandall, *Theory of Vibrating Systems and Sound* (Van Nostrand, New York, 1926).
[3]D. E. Weston, ''The theory of the propagation of plane sound waves in tubes,'' Proc. Phys. Soc. London, Sect. B **66**, 695 (1953).
[4]J. W. S. Rayleigh, *The Theory of Sound*, Vol. 2 (Macmillan, London, 1896).
[5]G. A. Bird, *Molecular Gas Dynamics and the Direct Simulation of Gas Flows* (Clarendon, Oxford, 1994).
[6]C. Cercignani, *The Boltzmann Equation and its Applications* (Springer-Verlag, New York, 1988).
[7]A. Beskok and G. E. Karniadakis, ''A model for flows in channels and ducts at micro and nano scales,'' Microscale Thermophys. Eng. **3**, 43 (1999).
[8]M. Knudsen, ''Die Gesetze der molecular Stromung und dieinneren Reibungstromung der Gase durch Rohren,'' Ann. Phys. (Leipzig) **28**, 75 (1909).
[9]T. Ohwada, Y. Sone, and K. Aoki, ''Numerical analysis of the Poiseuille and thermal transpiration flows between two parallel plates on the basis of the Boltzmann equation for hard-sphere molecules,'' Phys. Fluids A **1**, 2042 (1989).
[10]S. Fukui and R. Kaneko, ''Analysis of ultra thin gas film lubrication based on linearized Boltzmann equation: First report-derivation of a generalized lubrication equation including thermal creep flow,'' J. Tribol. **110**, 253 (1988).
[11]F. J. Alexander and A. L. Garcia, ''The direct simulation Monte Carlo method,'' Comput. Phys. **11**, 588 (1997).
[12]E. S. Oran, C. K. Oh, and B. Z. Cybyk, ''Direct simulation Monte Carlo: recent advances and applications,'' Annu. Rev. Fluid Mech. **30**, 403 (1998).
[13]F. Alexander, A. Garcia, and B. Alder, ''Cell size dependence of transport coefficients in stochastic particle algorithms,'' Phys. Fluids **10**, 1540 (1998); **12**, 731 (2000) (erratum).
[14]N. G. Hadjiconstantinou, ''Analysis of discretization in the direct simulation Monte Carlo,'' Phys. Fluids **12**, 2634 (2000).
[15]A. Garcia and W. Wagner, ''Time step truncation error in direct simulation Monte Carlo,'' Phys. Fluids **12**, 2621 (2000).
[16]The method is similar to the one presented in Ref. 19. However, due to a misprint, the positions of $A(x)$ and $B(x)$ in Eq. (1) of Ref. 19 have been reversed. The last part of Eq. (1) in Ref. 19 should be the same as in Eq. (23) of the present paper, i.e., $A(x)\cos \omega t + B(x)\sin \omega t$.
[17]W. H. Press, S. A. Teukolsky, W. T. Vetterling, and B. P. Flannery, *Numerical Recipes in C*, 2nd ed. (Cambridge University Press, Cambridge, 1992).
[18]L. D. Landau and E. M. Lifshitz, *Fluid Mechanics* (Pergamon, New York, 1989).
[19]N. G. Hadjiconstantinou and A. L. Garcia, ''Molecular simulations of sound wave propagation in simple gases,'' Phys. Fluids **13**, 1040 (2001).